

# Valence band splitting in $\text{Cu}_2(\text{Sn,Ge,Si})\text{S}_3$ : Effect on optical absorption spectra

Jessica de Wild\*, Efterpi Kalesaki, Ludger Wirtz, and Phillip J. Dale

Physics and Materials Science Research unit, University of Luxembourg, 162a Avenue de la Faïencerie,  
1511 Luxembourg, Luxembourg

Received 28 November 2016, revised 21 December 2016, accepted 27 December 2016  
Published online 9 January 2017

**Keywords** density functional theory, Wannier functions,  $\text{Cu}_2\text{SnS}_3$ ,  $\text{Cu}_2\text{GeS}_3$ ,  $\text{Cu}_2\text{SiS}_3$ , photovoltaics, optical absorption, valence band splitting

\* Corresponding author: e-mail [jessica.dewild@uni.lu](mailto:jessica.dewild@uni.lu)

We perform a detailed analysis of the valence band splitting (VBS) effect on the absorption spectra of monoclinic  $\text{Cu}_2(\text{Sn,Ge,Si})\text{S}_3$  combining theory and experiment. We calculate the imaginary part of the dielectric function for all three compounds using hybrid functionals and maximally localized Wannier functions in remarkably dense  $k$ -meshes to ensure an accurate description of the low energy spectral re-

gime. We find that the VBS will affect the absorption spectra of these materials leading to multiple absorption onsets. Our experimental spectra on  $\text{Cu}_2(\text{Sn,Ge})\text{S}_3$ , analysed using both Tauc plots and inflection points, verify this prediction. A good agreement between theory and experiment in terms of VBS values is recorded.

© 2017 WILEY-VCH Verlag GmbH & Co. KGaA, Weinheim

**1 Introduction**  $\text{Cu}_2(\text{Sn, Ge})\text{S}_3$  compounds have lately attracted interest as photovoltaic materials [1–3] due to their strong absorption in a wide range of the solar spectrum and their band gaps, which make them suitable for single or double junction solar cells.

An intriguing feature of these compounds, stemming from their reduced symmetry, i.e. monoclinic phase, is the splitting of the upper valence band (VB) states. Valence band splitting (VBS) is expected to affect the low energy regime of the absorption spectrum since transitions from all three upper VBs to the conduction band minimum (CBM) at the Brillouin zone center ( $\Gamma$ ) are allowed. The VBS effect on optical absorption has been discussed for the tetragonal  $\text{Cu}(\text{In,Ga})(\text{S,Se})_2$  compounds by Alonso et al. [4], who traced its origin to crystal field and spin orbit coupling; the latter found to play a more critical role in the case of selenides rather than sulfides. In their recent contribution, combining spectroscopic ellipsometry and theoretical calculations, Crovetto et al. discussed VBS as the origin of the double transition onset for  $\text{Cu}_2\text{SnS}_3$  (CTS) commonly observed in external quantum efficiency (EQE) measurements [5 and references therein]. However, no de-

tailed study has been performed on  $\text{Cu}_2\text{GeS}_3$  (CGS) or  $\text{Cu}_2\text{SiS}_3$  (CSiS). The differences and/or similarities in their absorption spectra originating by crystallographic structure, and chemical nature of the constituent elements are yet to be examined.

Most theoretical studies up to date were focused in correctly reproducing the band gap values of  $\text{Cu}_2(\text{Sn,Ge, Si})\text{S}_3$ . This was accomplished through the use of density functional theory (DFT) and hybrid functionals [6] or an onsite Coulomb potential term (DFT+U) [7, 8]. Attempts to correctly reproduce the low energy part of their optical spectra were hindered by the requirement for very dense  $k$ -grids, as recently shown for CTS [5]. The same was found to be true for the relevant  $\text{Cu}(\text{In,Ga})(\text{S,Se})_2$  compounds and was attributed to the strong dispersion of the conduction band states [9].

In our present contribution, we focus on the low energy regime and define the effect of VBS on the absorption spectra of  $\text{Cu}_2(\text{Sn,Ge,Si})\text{S}_3$ . Towards this goal we combine theoretical calculations on remarkably high  $k$ -meshes, and experimental results on optical absorption. Differences and similarities between the three compounds are highlighted.

**2 Theoretical determination of optical absorption spectra** We calculate the optical absorption spectra of monoclinic  $\text{Cu}_2(\text{Sn,Ge,Si})\text{S}_3$  close to the fundamental absorption edge. In all cases, DFT calculations are initially performed using the plane-wave projector augmented-wave (PAW) method [10, 11], and the Heyd–Scuseria–Ernzerhof hybrid functional [12] with a screening parameter of 0.2 Å (HSE06) [13] as implemented in the Vienna ab initio simulation package (VASP) [14]. In our work, structures are relaxed to their equilibrium geometry using the HSE06 functional. For CTS this results in a band gap value underestimated by 0.12 eV relative to that obtained with the experimental lattice constants [6]. All hybrid functional calculations are performed on a  $k$ -mesh of  $4 \times 4 \times 4$  for the primitive unit cells. We then interpolate the HSE eigenenergies and overlap matrices to finer  $k$ -grids using maximally localized Wannier functions [15, 16]. From the Wannier-interpolated bands and wave functions, we calculate the transition matrix elements and the optical absorption spectra in the independent particle approximation [16]. The  $\delta$ -functions in the joint density of states calculations are replaced by Fermi–Dirac smearing functions and we implement the adaptive broadening scheme proposed in Ref. [16] with a smearing prefactor  $\alpha$  of 0.5. The value of the prefactor is carefully chosen so that no spurious oscillations appear while at the same time the spectra are only moderately smoothed out. The optical absorption spectra presented in the following are obtained by interpolation in a  $300 \times 300 \times 300$   $k$ -mesh; a value easily accessible using Wannier functions and excluding any possibility of artificial effects. Note that in the sulfides examined here the splitting of the bands due to spin orbit coupling is negligible (order of  $10^{-2}$  meV). We therefore choose to omit spin orbit coupling from our study.

$\text{Cu}_2(\text{Sn,Ge,Si})\text{S}_3$  in their monoclinic phase (space group  $C_c$  or  $C_s^4$  in Schönflies notation, No. 9) are built by S atoms tetrahedrally bonded to Cu and (Ge,Sn,Si) atoms. The crystals comply with only two symmetry operations, i.e. the identity  $\{E\}$  and a horizontal mirror plane  $\{\sigma_h\}$ . The corresponding irreducible representations are the  $A'$  and  $A''$ , identity and parity representations, respectively. As a result of symmetry, the crystals are optically anisotropic and electron transitions at  $\Gamma$  from all three upper VBs to the CBM are allowed.

In Fig. 1(a) we present the HSE06 band structure of CGS. The band gap is calculated at 0.98 eV, which is underestimated with respect to the experimental value of 1.5 eV determined from a Tauc plot in absorption spectra [3]. A rough estimate for the band gap decrease at room temperature using the Varshni parameters would be of the order of 100 meV using the parameters of the relevant  $\text{Cu}_2\text{ZnSnS}_4$  compound [17]. The splitting of the valence bands is 0.12 and 0.14 eV from the topmost to the second and third VBs, respectively.

In Fig. 1(b) we present the mathematical average of the three components of the imaginary part of the dielectric function ( $\epsilon_2$ ), corresponding to the case of unpolarized

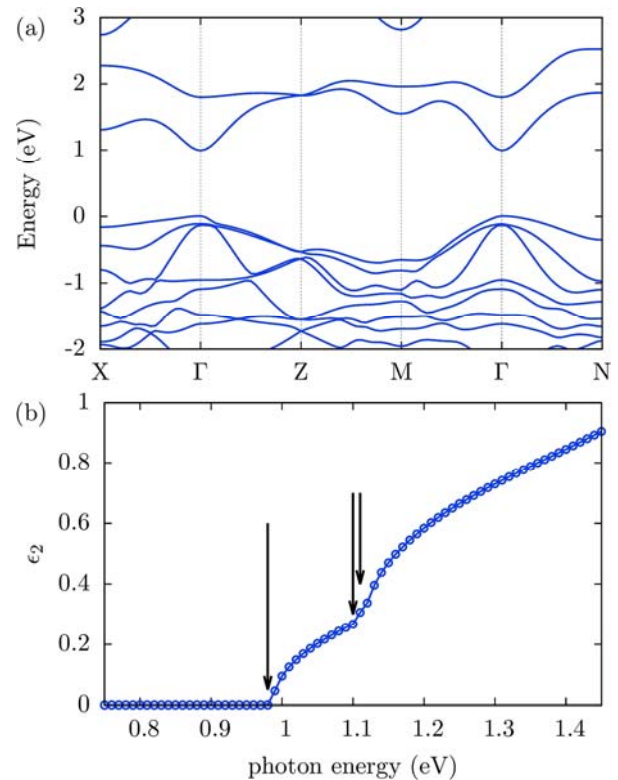


**Figure 1** (a) HSE06 band structure of  $\text{Cu}_2\text{GeS}_3$  (CGS), (b) mathematical average of the three components of the imaginary part of the dielectric function ( $\epsilon_2$ ). Arrows indicate the energies of the absorption onset and subsequent transitions right above the fundamental absorption edge.

light. Apparently two additional transitions occur right above the fundamental absorption edge, whose energy coincides with the gap values of the second and third VBs to the CBM at  $\Gamma$ . The energy of the latter is hardly discernible in the plots of Fig. 1(b) since the splitting between the second and third VBs is merely 0.02 eV. Note that for optical spectra calculations we used all VBs and only the lower two conduction bands (CBs) since the latter are disentangled from higher lying states. The inclusion of a reduced number of CB states is adequate for the present study since we are interested in correctly describing the low energy part of the spectrum.

In Figs. 2(a, c) we present the band structure and imaginary part of the dielectric function for CTS. The band gap of CTS is calculated at 0.76 eV, which is slightly underestimated with respect to the experimental value of 0.92 eV for the monoclinic phase [1, 18]. The splitting between the topmost and second VBs is found equal to 0.10 eV and the one between the topmost and third VBs is 0.15 eV. In accordance with the electronic structure, the absorption onset is traced at 0.76 eV in the plot of the imaginary part of the dielectric function. The subsequent,  $\Gamma$  related transitions at 0.86 eV and 0.91 eV are also evident and indicated by arrows in Fig. 2(c).

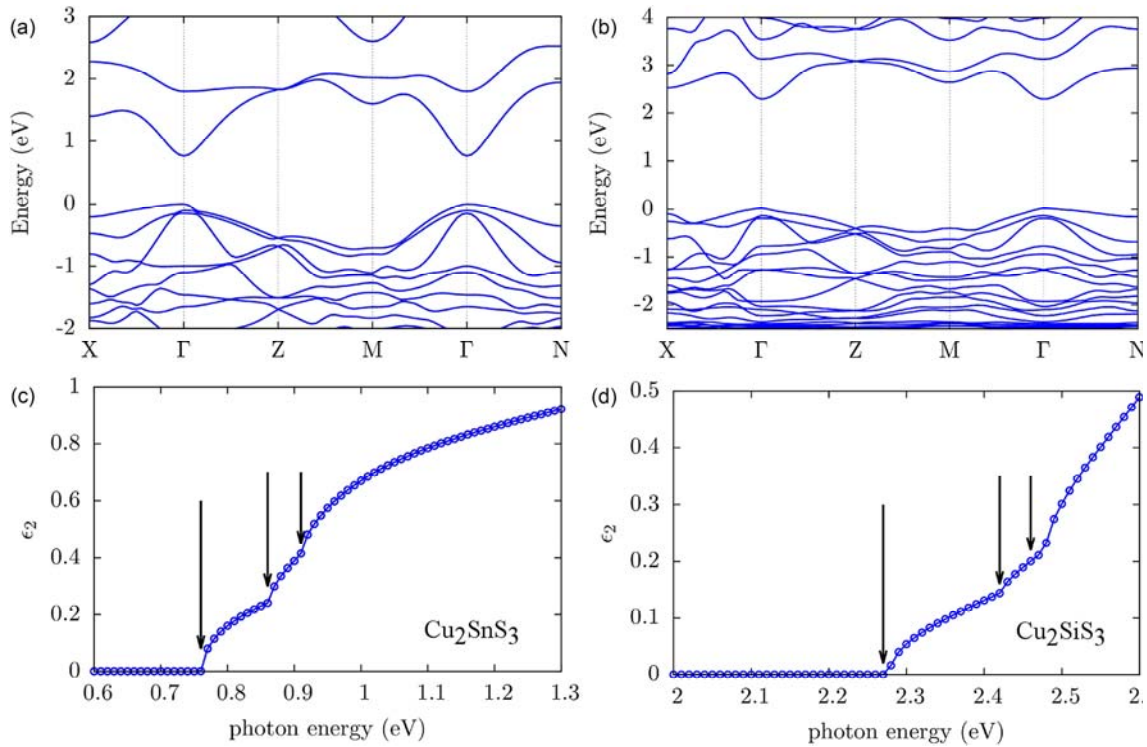


**Figure 2** HSE06 band structures and imaginary part of the dielectric functions for CTS (a, c) and CSiS (b, d). The transition energies right above the fundamental absorption edge, corresponding to transitions from the split upper VBs to the CBM at  $\Gamma$ , are indicated by arrows.

The third transition is more distinct in the case of CTS relative to CGS due to the greater splitting between the second and third VBs. We would therefore expect the triple onset to be more easily discernible in the absorption spectra of CTS rather than CGS, where a double onset would be observed. Preceding calculations by GW on top of DFT+U [8] for CTS and other compounds in the Cu–Sn–S family missed this triple transition characteristic due to the small  $k$ -grids used as also shown by Crovetto et al. [5].

Corresponding results for CSiS are illustrated in Fig. 2(b, d). Both electronic structure and  $\epsilon_2$  plots resemble those of CGS and CTS with an enhanced VBS. The band gap of CSiS is found equal to 2.27 eV. The second (third) VB is split off the topmost by 0.15 (0.20) eV.

Comparing the three compounds, we first observe that the band gaps decrease passing from Si- to Ge- to Sn. This trend is related to the increase in size of the constituent elements (3s orbitals in Si compared to 4s in Ge and 5s in Sn). The increase in atomic number leads to weaker bonding of Sn–S relative to Ge–S and Si–S and downshifts the CBM, which is built of S p – (Sn,Ge,S) s orbitals, leading to a band gap reduction.

The upper valence bands comprise in all cases Cu d and S p-orbitals at  $\Gamma$ . Our calculations show that VBS should be observed as a double/triple transition onset in the absorption spectra of all three compounds; the triple onset being more easily visible in the case of CTS and CSiS due

to the enhanced splitting between the second and third upper VBs.

In addition we find that the dielectric constant of CSiS is relatively low with respect to those of CGS, CTS. This feature and the high band gap of CSiS (1.82 eV [20]) establish the latter less interesting for photovoltaic applications. We therefore choose to focus on CGS and CTS in terms of experimental absorption spectra.

**3 Experimental absorption spectra** CTS and CGS absorber layers are prepared by coating ink containing  $\text{Sn}^{2+}$  and/or  $\text{Cu}^+$  ions on soda lime glass by blade coating. Precursors are annealed at 550 °C in Sn/S or Ge/S environments for 30 minutes. Under this methodology, Cu poor absorber layers are obtained and we have self-regulating Sn or Ge incorporation via the gas phase. Further details on samples' preparation, crystal phase, composition and morphology can be found in [18, 19]. Reflection and transmission spectra are measured with a LAMBDA 950 UV/Vis/NIR spectrophotometer with an integrating sphere. Absorption  $\alpha$  ( $\text{cm}^{-1}$ ) is determined from reflection ( $R$ ) and transmission ( $T$ ) measurements through

$$\alpha = -\frac{1}{d} \log \left( \frac{T}{1-R} \right), \quad (1)$$

where  $d$  is the thickness of the film. The thickness of our samples is approximately 1  $\mu\text{m}$ . Equation (1) is only valid

for the region where not all light is absorbed, which is the region of interest to us, i.e. near the band edge. Furthermore, the films are rough. Hence no interference fringes are observed in the spectra.

In the following, the band gap is determined from Tauc plots and compared with the inflection points. In Fig. 3(a) we show the absorption spectrum of the CGS film. Two transitions are clearly visible close to the onset. The derivative of the absorption spectrum (Fig. 3(b)) results in two distinct peaks, split by 0.13 eV. The inflection point maxima are at 1.55 eV and 1.68 eV, which are close to the band gap value of 1.55 eV and second transition at 1.65 eV reported by EQE measurements [3].

In Fig. 3(b) we also compare the derivative of the experimental spectrum to that obtained with DFT and Wannier functions having the theoretical spectrum shifted to match the experimental band gap value of 1.50 eV for CGS. In the derivative of the calculated spectrum two peaks are again visible with their maxima shifted to somewhat lower values but still retaining the same order of magnitude. The splitting in the calculated spectrum is 0.12 eV. The slight deviation in the value of the splitting between theory and experiment is due to the fact that the splitting between the second and third VBs is too small (0.02 eV). For that same reason, we cannot distinguish a third peak in the derivative plots of either experimental or theoretical data.

Figure 3(c) shows the corresponding Tauc plot for a direct band gap. The value extracted for the band gap is 1.51 eV, which is 0.04 eV lower than the value defined by the inflection points. The second transition cannot be determined from the Tauc plot, since it lies below the fundamental gap. However, in Ref. [3] the second transition was successfully determined from the absorption spectra and the second transition was 0.1 eV above the main gap. This is an indication that our sample suffers from enhanced tailing which can already be seen in the absorption spectra. The tailing could be due to the lower Cu/Ge ratio, the different processing of the precursor and/or the annealing method.

CTS shows slightly different results (Fig. 3(d–f)). The absorption spectrum of Fig. 3(d) and the corresponding derivative plot (Fig. 3(e)) show three peaks at 0.96, 1.07 eV and 1.12 eV. These resemble quite well the theoretically determined, crystal field split values of 0.10 eV and 0.15 eV, found also in the derivative plot of the theoretically defined  $\alpha$  (Fig. 3(e)). The latter is shifted to match the experimental band gap value of 0.92 eV [18]. The Tauc plot (Fig. 3(f)) gives values of 0.92 eV and 0.98 eV for the band gap and second transition, respectively, whereas the third transition cannot be determined. This was also the case in the Tauc plot analysis of ellipsometry data in Ref. [5]. We may thus conclude that Tauc plot analysis is not

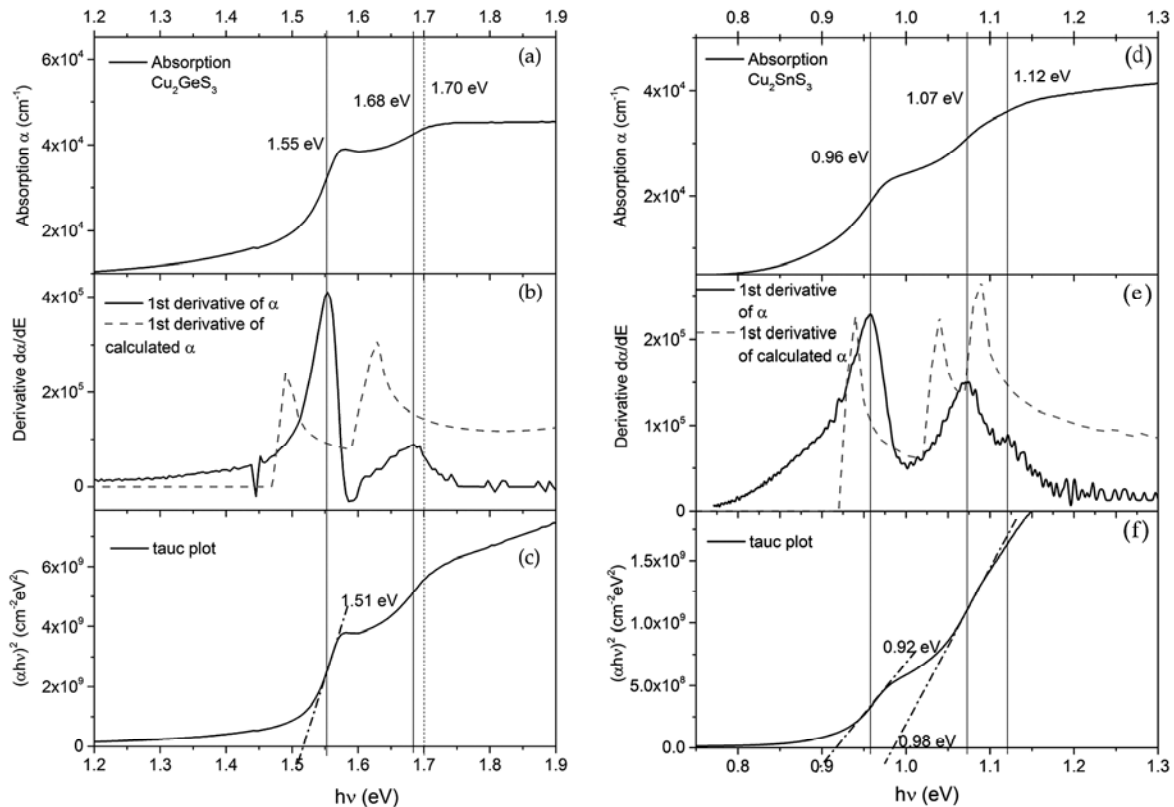


**Figure 3** (a) Experimental absorption spectrum, (b) inflection points compared with those calculated with DFT and Wannier functions, (c) Tauc plot of the experimental data for CGS. (d–f): Same graphs for CTS.

**Table 1** Transition energy values for CGS and CTS as defined by the inflection points of experimental absorption spectra, Tauc plots, our theoretical calculations shifted to match the experimental band gap values of [3] and [18], and reference external quantum efficiency (EQE) spectra.

		onset	2 <sup>nd</sup>	3 <sup>rd</sup>
CGS	inflection points	1.55	1.68	–
	Tauc plots	1.51	–	–
	theory	1.50	1.64	–
	EQE [3]	1.55	1.65	–
CTS	inflection points	0.96	1.07	1.12
	Tauc plots	0.92	0.98	–
	theory	0.92	1.02	1.07
	EQE [18]	0.93	0.99	–

sufficient to trace all features of the absorption spectra close to the fundamental edge for the currently examined compounds even when the splitting is large enough. Additional analysis with inflection points reveals the triple onset in CTS.

In Table 1 we collect the transition energy values presented for CGS and CTS. The fact that all three transitions are visible in the absorption spectra of CTS and two in CGS indicates that the material cannot be too distorted, since distortions would interfere with the positions of the valence bands. Indeed XRD analyses on our samples [18, 19] showed that the monoclinic phase is pure and not intermixed with cubic or other polymorphs.

**4 Conclusions** Our theoretical calculations using HSE06 functionals show that the upper VB states of monoclinic Cu<sub>2</sub>(Sn, Ge, Si)S<sub>3</sub> are split by approximately hundred meV due the reduced symmetry of the monoclinic phase. Using Wannier functions on top of DFT and remarkably high *k*-grids we find that VBS results in double/triple absorption onsets on the optical spectra of these materials since transitions from all three upper VBs to the CBM are allowed. Our findings are compared to the experimental spectra of CGS and CTS, which present high interest for photovoltaics. We carefully analyze these spectra using both inflection points and Tauc plots, and show that such a combined analysis is necessary to reveal all features of the absorption spectra close to the fundamental edge. Despite the large amount of tailing found, especially

for CGS, the transitions are in accordance with the theoretically predicted.

**Acknowledgements** E. K. and J. dW. contributed equally to this work. Calculations were carried out using the HPC facilities of the University of Luxembourg. E. K. and L. W. acknowledge support from the National Research Fund, Luxembourg, through Project No. C12/MS/3987081/TSDSN and J. dW and P. J. D through the FNR project EATSS n°C13/MS/5898466.

## References

- [1] A. Kanai, K. Toyonaga, K. Chino, H. Katagiri, and H. Araki, *Jpn. J. Appl. Phys.* **54**, 08KC06 (2015).
- [2] M. Umehara, S. Tajima, Y. Aoki, Y. Takeda, and T. Motohiro, *Appl. Phys. Express* **9**, 072301 (2016).
- [3] H. Araki, K. Chino, K. Kimura, N. Aihara, K. Jimbo, and H. Katagiri, *Jpn. J. Appl. Phys.* **53**, 05FW10 (2014).
- [4] M. I. Alonso, K. Wakita, J. Pascual, M. Garriga, and N. Yamamoto, *Phys. Rev. B* **63**, 075203 (2001).
- [5] A. Crovetto et al., *Sol. Energy Mater. Sol. Cells* **154**, 121–129 (2016).
- [6] A. Shigemi, T. Maeda, and T. Wada, *Phys. Status Solidi B* **252**, 1230–1234 (2015).
- [7] Y. Zhang et al., *J. Chem. Phys.* **139**, 184706 (2013).
- [8] P. Zawadzki et al., *Appl. Phys. Lett.* **103**, 253902 (2013).
- [9] S. Körbel et al., *Phys. Rev. B* **91**, 075134 (2015).
- [10] P. E. Blöchl, *Phys. Rev. B* **50**, 17953 (1994).
- [11] G. Kresse and D. Joubert, *Phys. Rev. B* **59**, 1758–1775 (1999).
- [12] J. Heyd, G. E. Scuseria, and M. Ernzerhof, *J. Chem. Phys.* **118**, 8207–8215 (2003).
- [13] A. V. Krukau, O. A. Vydrov, A. F. Izmaylov, and G. E. Scuseria, *J. Chem. Phys.* **125**, 224106 (2006).
- [14] G. Kresse and J. Furthmüller, *Comput. Mater. Sci.* **6**, 15 (1996).
- [15] A. A. Mostofi, J. R. Yates, Y.-S. Lee, I. Souza, D. Vanderbilt, and N. Marzari, *Comput. Phys. Commun.* **178**, 685–699 (2008).
- [16] J. R. Yates, X. Wang, D. Vanderbilt, and I. Souza, *Phys. Rev. B* **75**, 195121 (2007).
- [17] P. K. Sarswat and M. L. Free, *Physica B* **407**, 108 (2012).
- [18] J. de Wild, E. V. C. Robert, B. E. Adib, D. Abou-Ras, and P. J. Dale, *Sol. Energy Mater. Sol. Cells* **157**, 259–265 (2016).
- [19] E. V. C. Robert, J. de Wild, and P. J. Dale, *J. Alloys Compd.* **695**, 1307–1316 (2017).
- [20] H. ElAnzeery, M. Buffière, Kh. B. Messaoud, S. Oueslati, G. Brammert, O. El Daif, D. Cheyens, R. Guindi, M. Meuris, and J. Poortmans, *Phys. Status Solidi RRL* **9**, 338 (2015).